European Heart Journal – Cardiovascular Imaging (2014) **15**, 380–388
doi:10.1093/ehjci/jet251

Long-term effects of maximally intensive statin therapy on changes in coronary atheroma composition: insights from SATURN

Rishi Puri[1,2], Peter Libby[3], Steven E. Nissen[1], Kathy Wolski[2], Christie M. Ballantyne[4], Phillip J. Barter[5], M. John Chapman[6], Raimund Erbel[7], Joel S. Raichlen[8], Kiyoko Uno[9], Yu Kataoka[9], E. Murat Tuzcu[1], and Stephen J. Nicholls[3,9]*

[1]Department of Cardiovascular Medicine, Cleveland Clinic, Cleveland, OH, USA; [2]C5Research, Cleveland Clinic, Cleveland, OH, USA; [3]Cardiovascular Division, Brigham and Women's Hospital, Boston, MA, USA; [4]Section of Cardiovascular Research, Baylor College of Medicine and the Methodist DeBakey Heart and Vascular Center, Houston, TX, USA; [5]Heart Research Institute, Sydney, NSW, Australia; [6]INSERM Dyslipidaemia and Atherosclerosis Research Unit, Hôpital de la Pitié, Paris, France; [7]West German Heart Center, Essen, Germany; [8]AstraZeneca, Wilmington, DE, USA; and [9]South Australian Health and Medical Research Institute, University of Adelaide, Level 9, 121 King William Street, Adelaide, SA 5001, Australia

Received 20 July 2013; revised 11 October 2013; accepted after revision 8 November 2013; online publish-ahead-of-print 20 January 2014

Aims To evaluate the effect of long-term maximally intensive statin therapy on indices of coronary atheroma composition in a randomized trial, and how these changes relate to modifications of serum lipoproteins and systemic inflammation.

Methods and results The Study of coronary Atheroma by inTravascular Ultrasound: the effect of Rosuvastatin vs. atorvastatiN (SATURN) employed serial intravascular ultrasound (IVUS) measures of coronary atheroma in patients treated with rosuvastatin 40 mg or atorvastatin 80 mg daily for 24 months. Seventy-one patients underwent serial assessment of indices of plaque composition by spectral analysis of the radiofrequency IVUS signal. Changes in low-density lipoprotein cholesterol [LDL-C; −52 (−72, −33) mg/dL, $P < 0.001$], C-reactive protein [CRP −0.2 (−1, 0.1) mg/L, $P = 0.01$], and high-density lipoprotein cholesterol [HDL-C; +2.8 (−0.3, 7.8) mg/dL, $P < 0.001$] were associated with regression of percent atheroma volume (PAV: $-1.6 \pm 3.6\%$, $P < 0.001$). A reduction in estimated fibro-fatty tissue volume accompanied atheroma regression ($P < 0.001$), while dense calcium tissue volume increased ($P = 0.002$). There were no changes in fibrous or necrotic core tissue volumes. Volumetric changes in necrotic core tissue correlated with on-treatment HDL-C ($r = -0.27$, $P = 0.03$) and CRP ($r = 0.25$, $P = 0.03$) levels. A per-lesion analysis showed a reduction in the number of pathological intimal thickening lesions (defined by ≥3 consecutive IVUS frames containing PAV of ≥40%, predominantly fibro-fatty plaque, with <10% confluent necrotic core and <10% confluent dense calcium) at follow-up (67 vs. 38, $P = 0.001$). Fibroatheromas and fibrotic lesions remained static in number.

Conclusions Changes in indices of atheroma composition accompany regression of coronary atheroma with maximally intensive statin therapy, and associate with anti-inflammatory effects of statins.

ClinicalTrails.gov number NCT000620542.

Keywords Statins • Virtual Histology • IVUS • Atherosclerosis • Plaque composition

Introduction

High-intensity statin therapy lowers clinical event rates,[1] particularly in those at greatest cardiovascular risk. Coronary imaging studies have demonstrated the ability of statins to halt the progression of coronary atherosclerosis,[2,3] and to induce disease regression when the highest doses of the most effective statins are used.[4] Yet, the effects of maximally intensive statin treatment on human coronary atheroma composition remain unclear. Moreover, within the timeframe of follow-up, the degree of atheroma regression appears

* Corresponding author. Tel: +61 8 81164432, Email: stephen.nicholls@sahmri.com

more modest than the magnitude of clinical benefit accrued from statins, as well as the residual burden of disease that persists during therapy.

Pre-clinical studies have shown that statins possess pleiotropic effects distinct from their known lipoprotein-modulating properties.[5] The findings of statin-mediated reductions in inflammation in experimental atheroma[6] corroborated with the demonstration in humans that lower CRP levels in statin-treated patients associated with less coronary atheroma progression,[7] and better clinical outcomes,[8] than those with higher on-treatment CRP levels. Furthermore, statin-mediated increases in high-density lipoprotein cholesterol (HDL-C), in addition to substantial lowering of atherogenic lipoprotein levels, associate with net regression of coronary atheroma volume.[9] Hence, the particular interest in testing the long-term anti-atherosclerotic effects of maximally intensive statin therapy in intact humans, beyond measuring lesion size. The ability to undertake spectral analysis of the radiofrequency (RF) intravascular ultrasound (IVUS) signal allows assessment of indices of human coronary atheroma composition *in vivo*, with high reported accuracies.[10]

The Study of coronary Atheroma by inTravascular Ultrasound: the effect of Rosuvastatin vs. atorvastatiN (SATURN) compared directly the efficacy of two potent statin agents, each prescribed at their highest doses (rosuvastatin 40 mg daily vs. atorvastatin 80 mg daily), in altering the progression of coronary atherosclerosis over a 24-month period measured with serial IVUS.[11] A subset of patients enrolled in SATURN underwent collection of the serial RF-IVUS signal during protocol-specified IVUS imaging. This acquisition permitted testing the long-term effects of potent statin therapy on coronary atheroma composition and lesion phenotype, and how such changes may relate to alterations in serum lipoproteins and systemic inflammation.

Methods

Patient selection

The design of SATURN has been previously described.[11] Briefly, patients with angiographically demonstrable coronary disease and low-density lipoprotein cholesterol (LDL-C) <116 mg/dL, following a 2-week treatment period with atorvastatin (40 mg) or rosuvastatin (20 mg) daily, were re-randomized and treated for 24 months with atorvastatin (80 mg) or rosuvastatin (40 mg) daily. Subjects underwent IVUS imaging of a coronary artery at baseline and after 104 weeks of treatment.

Acquisition and analysis of intravascular coronary imaging

Entry criteria required the presence of at least one lumen stenosis $>20\%$ in an epicardial coronary artery at the time of a clinically indicated coronary angiogram. IVUS was performed at baseline in a single, native coronary artery with no lumen stenosis of $>50\%$, which had not undergone revascularization and was not considered to be the culprit vessel of a prior myocardial infarction. Images were screened by a core laboratory for a number of pre-specified requirements, and those patients whose baseline imaging met these requirements were eligible for randomization. Following 104 weeks of treatment, patients underwent a second IVUS of the same artery. Anatomically matched arterial segments were selected for analysis on the basis of proximal and distal fiduciary points. The analyses presented here pooled results from both treatment groups, as they did not differ in the primary endpoint of the trial.

The evaluation of serial changes in coronary atheroma composition as a function of on-treatment lipoprotein and inflammatory markers was a pre-specified exploratory endpoint of SATURN.[11] Centres equipped with IVUS console enabling acquisition of Virtual Histology® IVUS (VH-IVUS, Volcano Corp., Rancho Cordova, CA, USA) coronary imaging enrolled patients in SATURN. At these centres, serial IVUS was performed using a 45 MHz rotational catheter (Revolution, Volcano Corp.), optimized for RF data acquisition, at an automated pullback speed of 0.5 mm/s, following the administration of intracoronary nitroglycerine. During the catheter pullback, the RF signal was captured at the peak of the R-wave and stored onto DVDs. The captured RF signal enabled the reconstruction of a colour-coded map of coronary plaque composition, via the VH-IVUS algorithm, based on geometrically traced contours. The four RF colour-coded plaque components were red (indicating necrotic core), white (suggesting dense calcium), light green (designated fibro-fatty), and dark green (considered fibrotic) (*Figure 1*). Off-line grey-scale and VH-IVUS analysis was performed at the Atherosclerosis Imaging Core Laboratory, Cleveland Clinic, by analysts without knowledge of treatment assignments and temporal sequence of paired imaging, using echoPlaque 4.0 (Indec Medical Systems, Santa Clara, CA, USA). External elastic membrane (EEM) and lumen borders were contoured for each slice [median inter-slice distance 0.44 (0.41, 0.49) mm]. Plaque area was determined as the area between leading edges. On each frame, the acoustic shadow imparted by the rotational IVUS catheter had a mask assigned to it, and this area was excluded from analysis. At a vessel level, grey-scale plaque burden was calculated as percent atheroma volume (PAV) and total atheroma volume (TAV), as previously described.[4] Changes in PAV, TAV, lumen, and EEM volumes were calculated from measurements at 104 weeks minus the corresponding volume at baseline. Plaque regression was defined as any decrease in plaque burden from baseline. To assess atheroma composition, the absolute and relative (percentage) cross-sectional areas as defined by VH-IVUS parameters (fibro-fatty, fibrous, necrotic core, and dense calcium) were measured on each captured frame. The calculation of absolute and percentage-based volumes of each atheroma composition type per vessel was performed using the trapezoidal rule.[12]

To assess indices of lesion composition within each vessel at each time point, coronary plaques underwent classification according to the presence and distribution of RF-defined categories.[13–15] A lesion was defined by the presence of at least three consecutive frames that contained plaque burden of $\geq 40\%$. Lesions were considered separate if there was a minimum of 5 mm length of vessel containing no IVUS frame with measurable plaque burden of $\geq 40\%$. For the formal classification of each lesion, plaque burden (average atheroma area) and absolute tissue compositional volumes designated as fibro-fatty, fibrous, necrotic core, and dense calcium were calculated. Fibroatheromas (FAs) were defined as any lesion containing $\geq 10\%$ confluent necrotic core by VH criteria. Fibrotic (FIB) lesions contained mainly fibrous tissue with $<10\%$ necrotic core, $<15\%$ fibro-fatty, and $<10\%$ dense calcium tissue. FIB lesions with $\geq 10\%$ dense calcium were classified as calcified-FIB (FIB-Ca). Pathological intimal thickening (PIT) lesions consisted of predominantly ($\geq 15\%$) fibro-fatty tissue with $<10\%$ necrotic core and $<10\%$ dense calcium (*Figure 1*).

Statistical analysis

Categorical variables are summarized using frequencies and compared using the χ^2 test or Fisher's exact test, as appropriate. Continuous variables were summarized as means $\pm$ SD for variables with a normal distribution, and changes from baseline were tested with a paired *t*-test. Variables not following a normal distribution are presented as medians

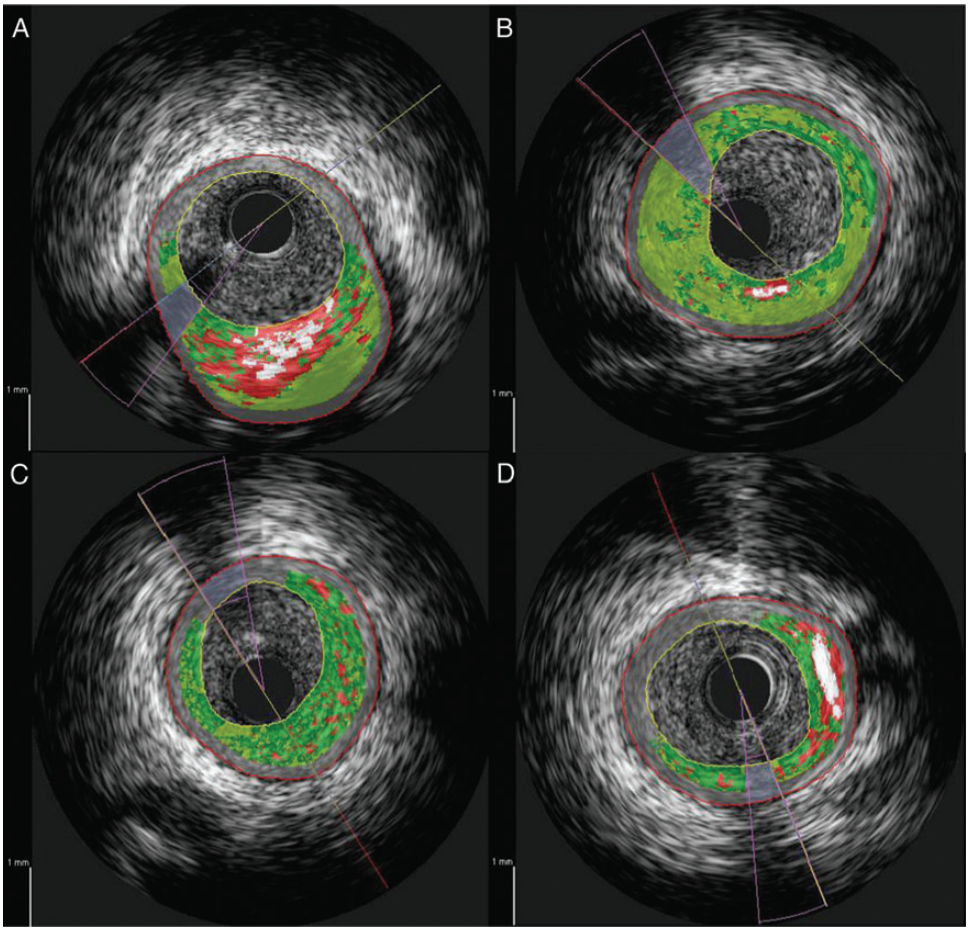

Figure 1 (*A*) Representative frame for an FA. PAV for this lesion was 60%. Relative tissue compositions were fibrous 26%, fibro-fatty 33%, necrotic core 32%, and dense calcium 9%. (*B*) Representative frame for a PIT lesion. PAV for this lesion was 68%. Relative tissue compositions were fibrous 33%, fibro-fatty 63%, necrotic core 3%, and dense calcium 1%. (*C*) Representative frame for an FIB lesion. PAV for this lesion was 62%. Relative tissue compositions were fibrous 75%, fibro-fatty 16%, necrotic core 9%, and dense calcium 0%. (*D*) Representative frame for an FIB-Ca lesion. PAV for this lesion was 52%. Relative tissue compositions were fibrous 57%, fibro-fatty 5%, necrotic core 25%, and dense calcium 13%. The area contained within the purple line refers to the mask applied to exclude plaque compositional analysis within the area of shadow imparted by the rotational IVUS catheter.

and inter-quartile range and tested using the Wilcoxon signed-rank test. Spearman correlation coefficients were generated between the RF-IVUS parameters, lipoprotein levels, and CRP levels. A simple linear regression model ($y = a + bx$) was created to describe the relationship between on-treatment HDL-C and CRP levels with change in necrotic core volume. The equation generated by this model was used to determine which levels of HDL-C and CRP corresponded with a change in necrotic core of ≤ 0. A *P*-value of <0.05 was considered statistically significant. The SAS software was used to perform all analyses (version 9.2, Cary, NC, USA).

Results

Patient characteristics

Of the 1385 randomized patients, 1039 underwent grey-scale IVUS imaging at baseline and follow-up. Of these, 71 patients had evaluable serial VH-IVUS imaging ($n = 36$ rosuvastatin and $n = 35$ atorvastatin). In SATURN, the primary efficacy endpoint of change in PAV did not differ significantly between the two treatment groups. Hence, this study combined data from the two treatment groups. *Table 1* summarizes baseline patient characteristics and concomitant medications of the population who underwent serial VH-IVUS imaging, which, in general, did not differ significantly from the characteristics of the overall SATURN population. Mean age was 57.6 ± 9.0 years, 80% were men, one-third of patients had either a prior history of myocardial infarction or coronary revascularization, 13% had diabetes mellitus, and 24% were current smokers.

Biochemical measurements

Table 2 presents baseline levels and changes in lipid variables and CRP. High-intensity statin therapy significantly reduced LDL-C, non-HDL-C, triglycerides, apolipoprotein B (ApoB), LDL-C:

HDL-C ratio, ApoB : apolipoprotein A-1 (ApoA-1) ratio, and CRP. HDL-C and ApoA-1 levels rose significantly.

Grey-scale and RF-IVUS analysis—volumetric vessel data

Table 3 describes the baseline, follow-up, and changes in grey-scale IVUS and RF-IVUS findings. Coronary atheromata regressed significantly, as measured by a change in PAV of $-1.6 \pm 3.6\%$ ($P < 0.001$). TAV also declined by -11.0 ± 23.3 mm^3 ($P < 0.001$). Lumen volume did not change significantly: -1.50 ± 34.1 mm^3 ($P = 0.48$), but the EEM volume decreased significantly: -12.6 ± 49.7 mm^3 ($P = 0.03$). Regression of PAV occurred in 68% (48 of 71 patients) of this population, whereas TAV declined in 76% (54 of 71 patients).

As maximally intensive statin therapy overall resulted in significant coronary atheroma regression, we report both the absolute and relative (percent) changes in indices of atheroma composition. Fibro-fatty tissue volume fell consistently [absolute change -4.8 (-14.9, -0.21) mm^3, $P < 0.001$; percent change -5.2% (-14.6, 3.6), $P = 0.002$], accompanied by a consistent increase in dense calcium tissue volume [absolute change $+0.32$ (-0.15, 1.2) mm^3, $P = 0.002$; percent change $+1.2\%$ (-0.33, 3.5), $P < 0.001$]. There was a reduction in absolute fibrous tissue volume [-2.2 (-9.0. 2.1) mm^3, $P < 0.001$], with no significant change in its relative (percent change) distribution [$+1.7\%$ (-6.1, 7.4), $P = 0.38$]. There was a non-significant absolute increase in necrotic core tissue volume [$+0.09$ (-1.2, 1.9) mm^3, $P = 0.84$], yet its relative distribution increased significantly [$+1.9\%$ (-0.44, 6.0), $P < 0.001$].

Table 1 Baseline patient demographics

Parameter	SATURN-VH (*N* = 71)	Main SATURN (*N* = 968)	*P*-value
Age (years)	57.6 ± 9.0	57.6 ± 8.5	0.95
Males (%)	80.3	73.1	0.18
BMI (kg/m^2)	28.6 ± 4.5	29.1 ± 5.3	0.42
Prior myocardial infarction (%)	32.4	23.8	0.11
Prior PCI or CABG (%)	33.8	22.7	0.03
Hypertension (%)	69.0	70.5	0.79
Diabetes (%)	12.7	15.5	0.53
Current smoker (%)	23.9	32.9	0.12
Anti-platelet therapy (%)	69.0	80.7	0.02
Beta-blockers (%)	59.2	61.0	0.76
ACEI (%)	47.9	43.8	0.50
ARB (%)	12.7	16.7	0.38
Nitrates (%)	80.3	82.9	0.58

Medications described are concomitant.
RF: radiofrequency; BMI: body mass index; PCI: percutaneous coronary intervention; CABG: coronary artery bypass surgery; ACEI: angiotensin-converting enzyme inhibitor; ARB: angiotensin receptor blocker; VH: Virtual Histology.

Grey-scale and VH-IVUS analysis—volumetric lesion data

Table 4 describes the type and number of VH-IVUS lesions at baseline and following high-intensity statin therapy. The numbers of FA (43 vs. 54, $P = 0.068$), FIB (18 vs. 26, $P = 0.12$), or FIB-Ca (2 vs. 4, $P = 0.43$) lesions did not differ significantly from baseline. The number of PIT lesions decreased significantly at follow-up (67 vs. 38, $P = 0.001$).

Relationships between on-treatment lipoprotein and inflammatory biomarker levels with volumetric changes in atheroma burden and composition

Table 5 describes the associations between time-weighted average (on-treatment) levels of serum lipoproteins and CRP with changes in atheroma burden and composition, following high-intensity statin therapy. Changes in PAV and on-treatment lipoprotein and CRP levels did not correlate. There was an inverse relationship between time-weighted average HDL-C levels and change in necrotic

Table 2 Baseline and serial changes in lipoprotein and CRP levels in all 71 patients

Parameter	Baseline	Follow-up	Change	*P*-value
Total cholesterol (mg/dL)	203.1 ± 38	146.2 ± 32.5	−56.9 ± 42.1	<0.001
LDL-C (mg/dL)	128.6 ± 30.7	72.4 ± 25.9	−56.2 ± 34.8	<0.001
HDL-C (mg/dL)	44.7 ± 11.0	48.2 ± 9.6	3.5 ± 7.1	<0.001
Non-HDL-C (mg/dL)	158.4 ± 36.5	98.0 ± 28.7	−60.4 ± 40.4	<0.001
Triglycerides (mg/dL)	130 (99, 191)	112 (94, 162)	−15 (−75, 16)	0.01
ApoA-1 (mg/dL)	133.3 ± 23.5	142.2 ± 20.8	8.4 ± 18.4	<0.001
ApoB (mg/dL)	106.3 ± 23.1	74.0 ± 20.0	−32.9 ± 24.4	<0.001
LDL-C : HDL-C	2.7 (2.4, 3.4)	1.5 (1.2, 1.9)	−1.4 (−1.9, −0.8)	<0.001
ApoB : ApoA-1	0.8 (0.7, 0.9)	0.5 (0.4, 0.6)	−0.3 (−0.4, −0.1)	<0.001
CRP (mg/L)	1.4 (0.7, 2.7)	1.0 (0.6, 1.9)	−0.2 (−1.0, 0.1)	0.01

Plus-minus values are mean ± SD; triglycerides, ratios of ApoB : ApoA-1, LDL : HDL, and CRP are reported as median (inter-quartile range).
CRP: C-reactive protein; LDL-C: low-density lipoprotein cholesterol; HDL-C: high-density lipoprotein cholesterol.

Table 3 Volumetric changes in grey-scale IVUS and VH-IVUS tissue components in all 71 patients

Volumetric parameter	Baseline	Follow-up	Change	*P*-value
Grey-scale IVUS				
PAV (%)	40.1 ± 8.8	38.5 ± 8.7	−1.58 ± 3.6	<0.001
TAV (mm^3)	146.0 ± 55.6	135.0 ± 50.9	−11.1 ± 23.3	<0.001
Lumen volume (mm^3)	214.9 ± 71.5	213.3 ± 72.5	−1.5 ± 34.1	0.48
EEM volume (mm^3)	360.9 ± 108.8	348.3 ± 105.4	−12.6 ± 49.7	0.03
VH-IVUS (absolute)				
Fibrous (mm^3)	18.5 (9.8, 29.3)	16.5 (5.9, 24.6)	−2.2 (−9.0, 2.1)	<0.001
Fibro-fatty (mm^3)	23.1 (8.8, 36.3)	13.4 (5.1, 28)	−4.8 (−14.9, −0.21)	<0.001
Dense calcium (mm^3)	1.2 (0.2, 3.8)	2.1 (0.3, 4)	0.32 (−0.15, 1.2)	0.002
Necrotic core (mm^3)	5.9 (2.6, 12.3)	6.0 (2.3, 12.4)	0.09 (−1.2, 1.9)	0.84
VH-IVUS (percent)				
Fibrous (%)	39 (32.7, 51.1)	40.3 (32.2, 49.8)	1.7 (−6.1, 7.4)	0.38
Fibro-fatty (%)	41.3 (31.5, 52.3)	36.6 (25.6, 47.5)	−5.2 (−14.6, 3.6)	0.002
Dense calcium (%)	2.1 (1.0, 7.0)	4.5 (1.6, 8.0)	1.2 (−0.03, 3.5)	<0.001
Necrotic core (%)	12.6 (8.2, 17.4)	15.5 (11.1, 19.3)	1.9 (−0.44, 6.0)	<0.001

Values are expressed as mean ± SD or median (IQR).
Tissue components are expressed as absolute volumes (mm^3) and as a percentage of total atheroma burden at each time point.
PAV: percent atheroma volume; TAV: total atheroma volume; VH: Virtual Histology.

Table 4 Lesion type and number by time point

Parameter, *n* (%)	Time point lesion number		*P*-value
	Baseline (*N* = 130)	Follow-up (*N* = 122)	
Fibroatheroma	43 (33.1)	54 (44.3)	0.068
Fibrotic	18 (13.9)	26 (21.3)	0.12
Calcified fibrotic	2 (1.5)	4 (3.3)	0.43
Pathological intimal thickening	67 (51.5)	38 (31.1)	0.001

core volume ($r = -0.27$, $P = 0.03$). *Figure 2* displays this finding as a linear regression line (with 95% confidence intervals). According to this relationship, HDL-C levels of >45.7 mg/dL associate with regression of necrotic core volume. On-treatment CRP levels related directly with changes in necrotic core volume ($r = 0.25$, $P = 0.03$) and also in DC volume ($r = 0.29$, $P = 0.01$). *Figure 3* displays a linear regression line (with 95% confidence intervals) between average on-treatment (log) CRP levels and change in necrotic core volume. According to this relationship, an average on-treatment CRP level of 1.43 mg/L or less associated with regression of necrotic core volume. Time-weighted average levels of LDL-C, triglyceride, ApoB, ApoA-1, LDL-C : HDL-C ratio, ApoB : ApoA-1 ratio did not associate with changes in atheroma composition.

Discussion

Statins favourably modulate atherogenic lipoprotein levels, and reduce primary and secondary cardiovascular events across a broad range of patient groups.[16] Yet, their modest effect on the absolute burden of atherosclerotic disease suggests that protective effects on the arterial wall may result, in part, from compositional changes rather than mere reduction in lesion size or the degree of stenosis.[17] In SATURN, significant lowering of atherogenic lipoprotein levels (LDL-C and ApoB), inflammatory status (CRP), and elevations of anti-atherogenic lipoproteins (HDL-C and ApoA-1) associated with overall atheroma regression, mediated largely by a reduction in the fibro-fatty tissue component, with less PIT lesions at follow-up. Although the studied vessels showed no overall change in necrotic core volume, changes in necrotic core volume associated inversely with on-treatment HDL-C levels, and directly with on-treatment CRP levels. These clinical observations correlate with animal experiments that demonstrated systemic lipid lowering by diet or statin administration reduced the lipid content and indicators of inflammation of atherosclerotic plaques.[18,19]

This SATURN sub-study provides serial volumetric coronary VH-IVUS imaging data from patients, with the longest duration of follow-up to date, who have undergone maximally intensive statin treatment. Prior imaging evaluations of statins on coronary lesion characteristics have often not involved the use of the highest doses of the most effective statins such as those employed here, nor for a prolonged treatment period.[19–25] Additionally, some of these prior studies evaluated much shorter coronary segments, with achieved LDL-C levels, significantly higher than those advocated by current treatment guidelines for patients with coronary artery disease.

Fibro-fatty tissue as categorized by VH-IVUS appears histologically to contain fibrous tissue, with surrounding foam cells or macrophages, indicative of an underlying inflammatory process, but with the absence of a prominent necrotic core.[26] *Ex vivo* post-mortem studies of advanced lesions causing fatal myocardial infarction

Table 5 Correlations between on-treatment lipoprotein and CRP levels with volumetric changes in atheroma composition

Parameter	Δ PAV		Δ Fibrotic		Δ Fibro-fatty		Δ Dense calcium		Δ Necrotic core	
	R	*P*-value	*R*	*P*-value	*R*	*P*-value	*R*	*P*-value	*R*	*P*-value
LDL-C	0.13	0.33	0.04	0.72	−0.004	0.97	−0.13	0.28	−0.07	0.55
HDL-C	0.05	0.67	−0.22	0.07	0.08	0.53	−0.05	0.69	−0.27	0.03
Trig	−0.03	0.81	−0.13	0.27	0.08	0.47	−0.15	0.21	−0.02	0.86
ApoB	0.07	0.58	0.02	0.89	−0.02	0.89	−0.11	0.36	−0.05	0.68
ApoA-1	0.03	0.80	−0.22	0.07	0.13	0.27	−0.01	0.93	−0.18	0.14
ApoB : ApoA-1	0.03	0.80	0.10	0.43	−0.11	0.35	−0.13	0.28	0.03	0.77
LDL : HDL	0.09	0.46	0.11	0.35	−0.07	0.54	−0.13	0.28	0.04	0.71
CRP	0.07	0.55	0.09	0.44	0.11	0.35	0.29	0.01	0.25	0.03

For lipoprotein, triglyceride, and CRP values, time-weighted average (on-treatment) values are reported.
For tissue components, Δ refers to the change in normalized volume from baseline.
R values are Spearman correlation coefficients.
Trig: triglycerides.

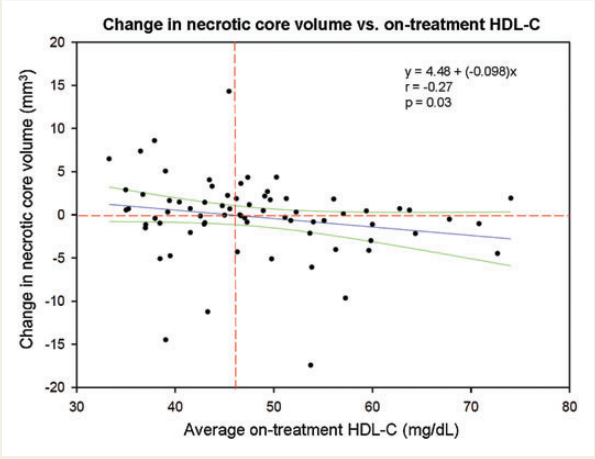

Figure 2 The relationship between change in necrotic core volume and on-treatment HDL-C levels, demonstrated by linear regression. Vertical dotted red line shows that HDL-C levels of >45.7 mg/dL associate with regression of necrotic core tissue volume.

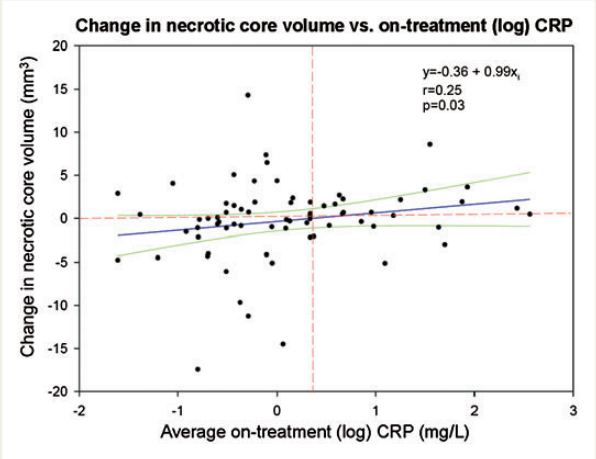

Figure 3 The relationship between change in necrotic core volume and on-treatment (log) CRP levels, demonstrated by linear regression. Vertical dotted red line shows that (log) CRP levels of >0.36 (translating into CRP of 1.43 mg/L) associate with increased necrotic core tissue volume.

enabled our current understanding of the role of atheroma composition in mediating lesion instability. The consistent demonstration of the presence of a large necrotic core in plaques that have disrupted and caused fatal myocardial infarction has thus far underscored the current proposed classification scheme of the so-called 'vulnerable' plaque, utilizing VH-IVUS.[27–29] This finding has stimulated a major focus on the utility of necrotic core tissue volume to serve as an imaging biomarker of coronary risk, which has, in-turn, spurred interest in developing therapeutic strategies that ameliorate necrotic core tissue volume. A prospective, observational study found that the presence of a VH-IVUS-derived thin-capped FA, containing >10% confluent necrotic core tissue volume, associated with clinical events.[30] Yet, most of the predictors of clinical events in this study pertained to the underlying burden of coronary atheroma, and subsequent lumen compromise. Thick-capped FAs were more prevalent than thin-capped FAs, equally prognostic of clinical events, yet seem not to have been incorporated into the multivariable model assessing various patient and lesion-level predictors of incident clinical events. It is, therefore, debatable as to whether the sub-categorization of FA via differing RF-IVUS algorithms yields incremental prognostic utility. Furthermore, the justification not to sub-categorize FA stems also from the fact that IVUS lacks the resolution to directly measure

fibrous cap thickness. Moreover, the proposed cut-point of ≥10% necrotic core volume to define FA on VH-IVUS is somewhat arbitrary and differs from the findings of prior autopsy studies.[27,31]

Our data suggest that the fibro-fatty component of established coronary atherosclerosis could represent a modifiable morphological compartment that contributes significantly towards high-intensity, statin-mediated coronary atheroma regression. The reduction in the number of PIT lesions, a less-advanced atheromatous lesion rich in fibro-fatty tissue, might also mean that such forms of atheromata are more susceptible to statin-mediated modification. Moreover, this change in the fibro-fatty content of plaque appears not to depend on achieved lipoprotein and CRP levels. Confirmation of this hypothesis will require further prospective clinical evaluation in a larger patient cohort.

Despite significant atheroma regression, we found that the amount of dense calcium tissue increased modestly following 2 years of intensive statin therapy. We also found a direct relationship between the change in volume of dense calcium tissue and on-treatment CRP levels. Others have also described increases in atheroma calcification on serial RF imaging following statin therapy.[22,24,25] More recently, Nakazato *et al.*[32] found an association between statin use and an increased prevalence of coronary plaque calcification on computed tomography coronary angiography. Most consider atheroma calcification to indicate advanced atherosclerotic disease, and a large pathological study has described a direct correlation between the vessel volumes of total atheroma and calcium.[33] A serial observation of increasing atheroma calcification, despite net statin-mediated atheroma regression, therefore seems somewhat paradoxical. Yet, the pattern and distribution of calcification appears to be critical in its association with the acuity of clinical presentation of coronary artery disease. Spotty calcification more frequently associates with the presence of culprit lesions causing acute coronary syndromes,[34,35] compared with stable coronary syndromes, and also associates with accelerated disease progression.[36] Indeed, if statin treatment rendered lesion microcalcifications more confluent, computational analyses suggest that vessel wall stresses could fall substantially.[37] Atherosclerosis involves a number of cellular mediators common to osteogenesis and bone mineralization.[38] Inflammatory cytokines induce ostegenic changes within the arterial wall,[39,40] which may explain our findings of a direct association between the change in dense calcium tissue volume and on-treatment CRP levels. Indeed, statins can exert paradoxical effects on cellular calcification pathways *in vivo*.[41] As such, the underlying mechanisms of statin-mediated changes in vascular calcification and their clinical significance warrant further investigation.

Inflammation participates in all stages of atherogenesis.[42] On histological analysis, necrotic core tissue contains cellular debris derived from dead lipid-laden macrophages, smooth muscle cells, trapped red blood cells, and fibrin, with surrounding microcalcification,[43] most of which link to a localized inflammatory reaction. The lack of collagen and tissue matrix, and abundant cholesterol, results in poor biomechanical stability, and punctate calcium mineral deposits can render such focal regions susceptible to rupture. We observed no consistent change in necrotic core volume following maximally intensive statin therapy. We did, however, find a direct relationship between on-treatment CRP levels and changes in necrotic core volume, indicating that, on average, patients prescribed potent statin therapy who did not achieve CRP lowering, experienced necrotic core expansion. A post hoc analysis from the Reversal of Atherosclerosis with Aggressive Lipid Lowering (REVERSAL) trial showed that greater reductions in CRP independently associated with a reduced rate of coronary disease progression, following intensive statin treatment.[7] In parallel, a pre-specified analysis of the Pravastatin or Atorvastatin Evaluation and Infection Therapy (PROVE-IT) demonstrated that, at all levels of achieved LDL-C, lower on-treatment CRP levels associated with lower clinical events.[8] REVERSAL, however, did not assess serial changes in plaque composition.

HDL-C levels correlate inversely with cardiovascular event rates,[44] and HDL particles can possess anti-inflammatory properties.[45] We observed an inverse relationship between on-treatment HDL-C levels and change in necrotic core volume. This finding could indicate that individuals with low on-treatment HDL-C levels and established coronary artery disease have residual coronary plaque inflammation. Infusions of recombinant HDL in patients with acute coronary syndrome resulted in acute atheroma regression.[46] Furthermore, HDL functionality, independent of the level of HDL-C, relates to the underlying burden of atherosclerotic disease.[47] Understanding the mechanistic association between therapies that elevate HDL-C levels, modulate HDL particle functionality, and subsequent change in atheroma burden and composition will require further study.

The current analysis has several limitations. SATURN was not a placebo-controlled study, precluding the possibility of direct comparison of these results to the natural history of atherosclerosis in such patients. Statins however, remain the backbone of our current armamentarium of anti-atherosclerotic therapies, limiting the ethics and feasibility of conducting future natural history trials of atherosclerosis in coronary artery disease patients without background statin therapy. SATURN imaged non-critically diseased, non-culprit vessels, limiting the extrapolation of the present findings to the biology of angiographically critical lesions. The PROSPECT study, however, found that half of all clinical events stemmed from non-culprit atheroma, outlining the systemic nature of disease.[30] Although accurate matching of serial IVUS pullbacks occurred via co-registration of anatomical landmarks, VH-IVUS has limited longitudinal resolution owing to electrocardiography-triggered image acquisition. This feature may have biased the precise serial matching of frames during lesion-based analysis, although whole-vessel volumetric analysis might reduce this concern. The halo surrounding dense calcium tissue can artificially overestimate RF-defined necrotic core tissue. Given our observation of an increase in dense calcium tissue volume, this known artefact might have caused overestimation of necrotic core tissue volume.[48] All VH-IVUS data, in SATURN, were captured with the 45 MHz rotational catheter, however, the formal validation of VH on this higher-resolution (Revolution) catheter has yet to be formally published. Moreover, VH-IVUS in its present state of validation has limited ability to resolve the fibrous from the fatty (lipidic) component in lesions categorized as fibro-fatty; found here to diminish with statin treatment. In addition, a number of studies utilizing a range of invasive and non-invasive imaging technologies reported differing effects of statins on plaque composition in a range of arterial beds. Therefore, it is likely that more sophisticated imaging tools, including a more robust validation

of these techniques, will be necessary to better elucidate mechanisms underlying statin (and non-statin)-mediated alterations of atheroma *in vivo*. Ultimately, the prognostic significance for assessing plaque composition needs more rigorous testing in larger, prospective, well-designed clinical trials.

In summary, maximally intensive statin therapy, prescribed for 24 months, results in coronary atheroma regression. This study indicates that this treatment reduces the fibro-fatty component of plaques, and increases dense calcium tissue. Changes in necrotic core volume correlated directly with systemic inflammation and inversely with on-treatment HDL-C levels. These results provide novel insights into the mechanisms, whereby statins influence the biology of plaques related to their propensity to provoke clinical atherothrombotic events.

Acknowledgements

We would like to acknowledge all staff of the Atherosclerosis Imaging Core Laboratory for undertaking of this analysis.

Conflict of interest: none declared.

References

1. Baigent C, Blackwell L, Emberson J, Holland LE, Reith C, Bhala N *et al.* Efficacy and safety of more intensive lowering of LDL cholesterol: a meta-analysis of data from 170,000 participants in 26 randomised trials. *Lancet* 2010;**376**:1670–81.
2. Nissen SE, Tuzcu EM, Schoenhagen P, Brown BG, Ganz P, Vogel RA *et al.* Effect of intensive compared with moderate lipid-lowering therapy on progression of coronary atherosclerosis: a randomized controlled trial. *JAMA* 2004;**291**:1071–80.
3. Nissen SE, Nicholls SJ, Sipahi I, Libby P, Raichlen JS, Ballantyne CM *et al.* Effect of very high-intensity statin therapy on regression of coronary atherosclerosis: the ASTEROID trial. *JAMA* 2006;**295**:1556–65.
4. Nicholls SJ, Ballantyne CM, Barter PJ, Chapman MJ, Erbel RM, Libby P *et al.* Effect of two intensive statin regimens on progression of coronary disease. *N Engl J Med* 2011; **365**:2078–87.
5. Takemoto M, Liao JK. Pleiotropic effects of 3-hydroxy-3-methylglutaryl coenzyme a reductase inhibitors. *Arterioscler Thromb Vasc Biol* 2001;**21**:1712–9.
6. Aikawa M, Rabkin E, Sugiyama S, Voglic SJ, Fukumoto Y, Furukawa Y *et al.* An HMG-CoA reductase inhibitor, cerivastatin, suppresses growth of macrophages expressing matrix metalloproteinases and tissue factor in vivo and in vitro. *Circulation* 2001;**103**:276–83.
7. Nissen SE, Tuzcu EM, Schoenhagen P, Crowe T, Sasiela WJ, Tsai J *et al.* Statin therapy, LDL cholesterol, C-reactive protein, and coronary artery disease. *N Engl J Med* 2005; **352**:29–38.
8. Ridker PM, Cannon CP, Morrow D, Rifai N, Rose LM, McCabe Ch *et al.* C-reactive protein levels and outcomes after statin therapy. *N Engl J Med* 2005; **352**:20–8.
9. Nicholls SJ, Tuzcu EM, Sipahi I, Grasso AW, Schoenhagen P, Hu T *et al.* Statins, high-density lipoprotein cholesterol, and regression of coronary atherosclerosis. *JAMA* 2007;**297**:499–508.
10. Nair A, Kuban BD, Tuzcu EM, Schoenhagen P, Nissen SE, Vince DG. Coronary plaque classification with intravascular ultrasound radiofrequency data analysis. *Circulation* 2002;**106**:2200–6.
11. Nicholls SJ, Borgman M, Nissen SE, Raichlen JS, Ballantyne C, Barter P *et al.* Impact of statins on progression of atherosclerosis: rationale and design of SATURN (Study of coronary Atheroma by inTravascular Ultrasound: effect of Rosuvastatin vs atorvastatiN). *Curr Med Res Opin* 2011;**27**:1119–29.
12. Atkinson KE. *An Introduction to Numerical Analysis.* 2nd ed. New York: John Wiley and Sons; 1989.
13. Garcia-Garcia HM, Mintz GS, Lerman A, Vince DG, Margolis MP, van Es GA *et al.* Tissue characterisation using intravascular radiofrequency data analysis: recommendations for acquisition, analysis, interpretation and reporting. *EuroIntervention* 2009; **5**:177–89.
14. Kubo T, Maehara A, Mintz GS, Doi H, Tsujita K, Choi SY *et al.* The dynamic nature of coronary artery lesion morphology assessed by serial virtual histology intravascular ultrasound tissue characterization. *J Am Coll Cardiol* 2010;**55**:1590–7.
15. Maehara A, Cristea E, Mintz GS, Lansky AJ, Dressler O, Biro S *et al.* Definitions and methodology for the grayscale and radiofrequency intravascular ultrasound and coronary angiographic analyses. *JACC Cardiovasc Imaging* 2012;**5**:S1–9.
16. Vaughan CJ, Gotto AM Jr, Basson CT. The evolving role of statins in the management of atherosclerosis. *J Am Coll Cardiol* 2000;**35**:1–10.
17. Libby P, Aikawa M. Mechanisms of plaque stabilization with statins. *Am J Cardiol* 2003; **91**:4B–8B.
18. Aikawa M, Rabkin E, Okada Y, Voglic SJ, Clinton SK, Brinckerhoff CE *et al.* Lipid lowering by diet reduces matrix metalloproteinase activity and increases collagen content of rabbit atheroma: a potential mechanism of lesion stabilization. *Circulation* 1998;**97**:2433–44.
19. Crisby M, Nordin-Fredriksson G, Shah PK, Yano J, Zhu J, Nilsson J. Pravastatin treatment increases collagen content and decreases lipid content, inflammation, metalloproteinases, and cell death in human carotid plaques: implications for plaque stabilization. *Circulation* 2001;**103**:926–33.
20. Underhill HR, Yuan C, Zhao XQ, Kraiss LW, Parker DL, Saam T *et al.* Effect of rosuvastatin therapy on carotid plaque morphology and composition in moderately hypercholesterolemic patients: a high-resolution magnetic resonance imaging trial. *Am Heart J* 2008;**155**:584, e1–8.
21. Okazaki S, Yokoyama T, Miyauchi K, Shimada K, Kurata T, Sato H *et al.* Early statin treatment in patients with acute coronary syndrome: demonstration of the beneficial effect on atherosclerotic lesions by serial volumetric intravascular ultrasound analysis during half a year after coronary event: the ESTABLISH Study. *Circulation* 2004;**110**:1061–8.
22. Kawasaki M, Sano K, Okubo M, Yokoyama H, Ito Y, Murata I *et al.* Volumetric quantitative analysis of tissue characteristics of coronary plaques after statin therapy using three-dimensional integrated backscatter intravascular ultrasound. *J Am Coll Cardiol* 2005;**45**:1946–53.
23. Nasu K, Tsuchikane E, Katoh O, Tanaka N, Kimura M, Ehara M *et al.* Effect of fluvastatin on progression of coronary atherosclerotic plaque evaluated by virtual histology intravascular ultrasound. *JACC Cardiovasc Intervent* 2009;**2**:689–96.
24. Hong MK, Park DW, Lee CW, Lee SW, Kim YH, Kang DH *et al.* Effects of statin treatments on coronary plaques assessed by volumetric virtual histology intravascular ultrasound analysis. *JACC Cardiovasc Intervent* 2009;**2**:679–88.
25. Eshtehardi P, McDaniel MC, Dhawan SS, Binongo JN, Krishnan SK, Golub L *et al.* Effect of intensive atorvastatin therapy on coronary atherosclerosis progression, composition, arterial remodeling, and microvascular function. *J Invasive Cardiol* 2012;**24**:522–9.
26. Nair A, Margolis MP, Kuban BD, Vince DG. Automated coronary plaque characterisation with intravascular ultrasound backscatter: ex vivo validation. *EuroIntervention* 2007;**3**:113–20.
27. Kolodgie FD, Virmani R, Burke AP, Farb A, Weber DK, Kutys R *et al.* Pathologic assessment of the vulnerable human coronary plaque. *Heart* 2004;**90**:1385–91.
28. Schaar JA, Muller JE, Falk E, Virmani R, Fuster V, Serruys PW *et al.* Terminology for high-risk and vulnerable coronary artery plaques. Report of a meeting on the vulnerable plaque, June 17 and 18, 2003, Santorini, Greece. *Eur Heart J* 2004;**25**: 1077–82.
29. Rodriguez-Granillo GA, Garcia-Garcia HM, Mc Fadden EP, Valgimigli M, Aoki J, de Feyter P *et al.* In vivo intravascular ultrasound-derived thin-cap fibroatheroma detection using ultrasound radiofrequency data analysis. *J Am Coll Cardiol* 2005;**46**: 2038–42.
30. Stone GW, Maehara A, Lansky AJ, de Bruyne B, Cristea E, Mintz GS *et al.* A prospective natural-history study of coronary atherosclerosis. *N Engl J Med* 2011;**364**: 226–35.
31. Falk E, Wilensky RL. Prediction of coronary events by intravascular imaging. *JACC Cardiovasc Imaging* 2012;**5**:S38–41.
32. Nakazato R, Gransar H, Berman DS, Cheng VY, Lin FY, Achenbach S *et al.* Statins use and coronary artery plaque composition: results from the International Multicenter CONFIRM Registry. *Atherosclerosis* 2012;**225**:148–53.
33. Sangiorgi G, Rumberger JA, Severson A, Edwards WD, Gregoire J, Fitzpatrick LA *et al.* Arterial calcification and not lumen stenosis is highly correlated with atherosclerotic plaque burden in humans: a histologic study of 723 coronary artery segments using nondecalcifying methodology. *J Am Coll Cardiol* 1998;**31**:126–33.
34. Ehara S, Kobayashi Y, Yoshiyama M, Shimada K, Shimada Y, Fukuda D *et al.* Spotty calcification typifies the culprit plaque in patients with acute myocardial infarction: an intravascular ultrasound study. *Circulation* 2004;**110**:3424–9.
35. Motoyama S, Kondo T, Sarai M, Sugiura A, Harigaya H, Sato T *et al.* Multislice computed tomographic characteristics of coronary lesions in acute coronary syndromes. *J Am Coll Cardiol* 2007;**50**:319–26.
36. Kataoka Y, Wolski K, Uno K, Puri R, Tuzcu EM, Nissen SE *et al.* Spotty calcification as a marker of accelerated progression of coronary atherosclerosis: insights from serial intravascular ultrasound. *J Am Coll Cardiol* 2012;**59**:1592–7.
37. Maldonado N, Kelly-Arnold A, Vengrenyuk Y, Laudier D, Fallon JT, Virmani R *et al.* A mechanistic analysis of the role of microcalcifications in atherosclerotic plaque stability: potential implications for plaque rupture. *Am J Physiol Heart Circ Physiol* 2012;**303**:H619–28.

38. Bostrom K, Watson KE, Horn S, Wortham C, Herman IM, Demer LL. Bone morphogenetic protein expression in human atherosclerotic lesions. *J Clin Invest* 1993;**91**:1800–9.
39. Hirota S, Imakita M, Kohri K, Ito A, Morii E, Adachi S *et al.* Expression of osteopontin messenger RNA by macrophages in atherosclerotic plaques. A possible association with calcification. *Am J Pathol* 1993;**143**:1003–8.
40. Aikawa E, Nahrendorf M, Figueiredo JL, Swirski FK, Shtatland T, Kohler RH *et al.* Osteogenesis associates with inflammation in early-stage atherosclerosis evaluated by molecular imaging in vivo. *Circulation* 2007;**116**:2841–50.
41. Wu B, Elmariah S, Kaplan FS, Cheng G, Mohler ER III. Paradoxical effects of statins on aortic valve myofibroblasts and osteoblasts: implications for end-stage valvular heart disease. *Arterioscler Thromb Vasc Biol* 2005;**25**:592–7.
42. Libby P. Inflammation in atherosclerosis. *Arterioscler Thromb Vasc Biol* 2012;**32**:2045–51.
43. Virmani R, Burke AP, Farb A, Kolodgie FD. Pathology of the vulnerable plaque. *J Am Coll Cardiol* 2006;**47**:C13–8.
44. Gordon DJ, Probstfield JL, Garrison RJ, Neaton JD, Castelli WP, Knoke JD *et al.* High-density lipoprotein cholesterol and cardiovascular disease. Four prospective American studies. *Circulation* 1989;**79**:8–15.
45. Barter PJ, Nicholls S, Rye KA, Anantharamaiah GM, Navab M, Fogelman AM. Antiinflammatory properties of HDL. *Circ Res* 2004;**95**:764–72.
46. Nissen SE, Tsunoda T, Tuzcu EM, Schoenhagen P, Cooper CJ, Yasin M *et al.* Effect of recombinant ApoA-I Milano on coronary atherosclerosis in patients with acute coronary syndromes: a randomized controlled trial. *JAMA* 2003;**290**:2292–300.
47. Khera AV, Cuchel M, de la Llera-Moya M, Rodrigues A, Burke MF, Jafri K *et al.* Cholesterol efflux capacity, high-density lipoprotein function, and atherosclerosis. *N Engl J Med* 2011;**364**:127–35.
48. Sheet D, Karamalis A, Eslami A, Noel P, Virmani R, Nakano M *et al.* Hunting for necrosis in the shadows of intravascular ultrasound. *Comput Med Imaging Graph* 2013 doi:10.1016/j.compmedimag.2013.08.002.

IMAGE FOCUS

doi:10.1093/ehjci/jet193
Online publish-ahead-of-print 18 October 2013

Combined subaortic membrane and aortic valve stenosis: additive value of three-dimensional echocardiography

Jose Alberto de Agustin*, Jose Juan Gomez de Diego, Pedro Marcos-Alberca, Carlos Macaya, and Leopoldo Perez de Isla

Cardiovascular Institute, Hospital Universitario San Carlos, Profesor Martin Lagos s/n, Madrid 28040, Spain

* Corresponding author. Tel: +34 913303394; Fax: +34 913303290, Email: albertutor@hotmail.com

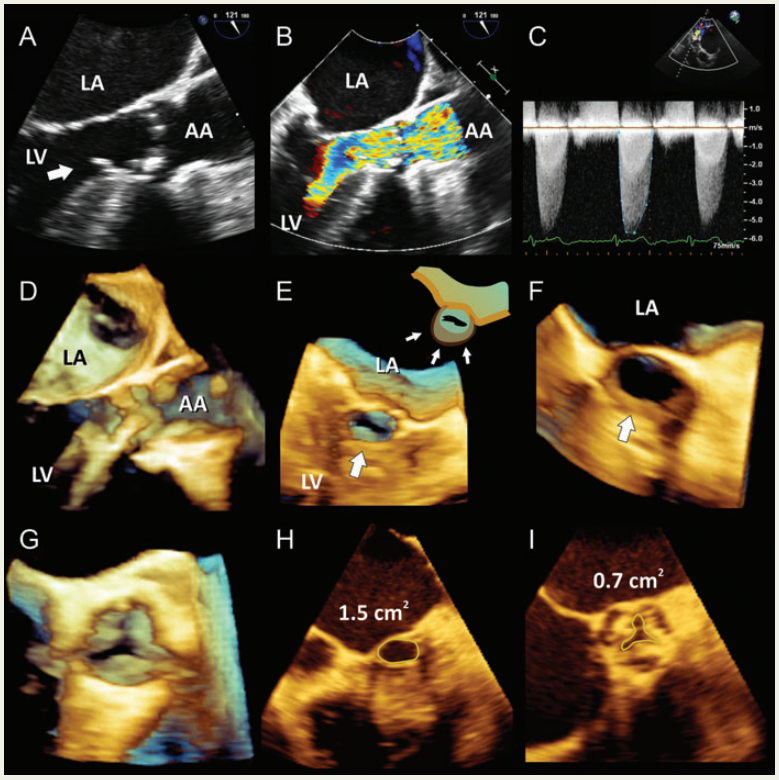

A 75-year-old woman was referred to our hospital for further assessment of undefined transaortic high-pressure gradient obtained by transthoracic echocardiography. Transoesophageal echocardiography revealed the presence of a subaortic membrane co-existing with aortic valve stenosis (*Panel A*, see Supplementary data online, *Video S1*). Colour flow and continuous-wave Doppler echocardiography (*Panels B and C*) demonstrated an increased aortic jet velocity of 5.7 m/s. Pulsed wave Doppler recording of the outflow area showed a mosaic pattern indicative of high subaortic flow velocities. Live three-dimensional echocardiography was performed, which improved the spatial assessment of the subaortic membrane (*Panel D*, see Supplementary data online, *Video S2*), including direct en face visualization from the left ventricular cavity (*Panel E*, see Supplementary data online, *Video S3*) and through a plane immediately below the aortic valve (*Panel F*, see Supplementary data online, *Video S4*). The membrane was circumferential and its attachment to both the ventricular septum and the anterior mitral leaflet was clearly demonstrated. En face view of the aortic valve from the ascending aorta was also obtained (*Panel G*, see Supplementary data online, *Video S5*). A multiplanar review mode was used to perform the planimetry of both the subvalvular and valvular stenotic areas, resulting 1.5 cm^2 at the level of the membrane during systole (*Panel H*), indicative of no significant obstruction, while at the level of the aortic valve cusps was 0.7 cm^2 (*Panel I*), consistent with severe aortic valve stenosis. This report shows the usefulness of three-dimensional echocardiography in combined valvular and subvalvular obstruction, where Doppler-derived methods are limited.

Supplementary data are available at *European Heart Journal – Cardiovascular Imaging* online.